Supporting information

Significantly improved stability and water retention for Pt supported on W-doped SnO_2 to catalyse the oxygen reduction reaction in proton exchange membrane fuel cells

Wei Cao,[a,c] Yiyang Mao,[a,c] Bin Hu,[a] Yongqing Yang,[a] Wei Zhou,[a]* and Zongping Shao[a,b]*

[a]*State Key Laboratory of Materials-Oriented Chemical Engineering, College of Chemical Engineering, Nanjing Tech University, Nanjing, 210009, China*

[b]*Department of Chemical Engineering, Curtin University, Perth, 6845, Australia*

[c]*These authors contributed equally to this work.*

**Corresponding Author*

Corresponding Author

*E-mail: zhouwei1982@njtech.edu.cn (W.Z.)

*E-mail: shaozp@njtech.edu.cn (Z.S.)

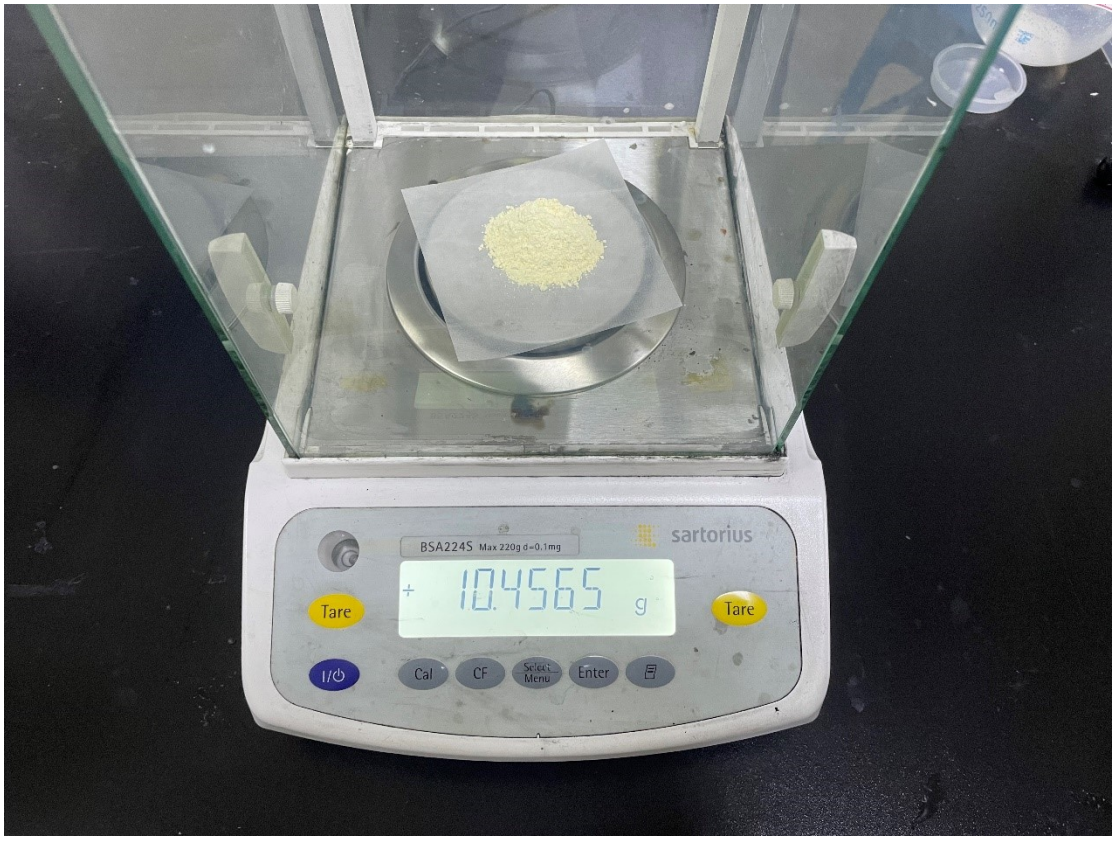

Supplementary Figure. 1 Sample $W_{0.02}$-SnO_2 prepared in mass production (10g)

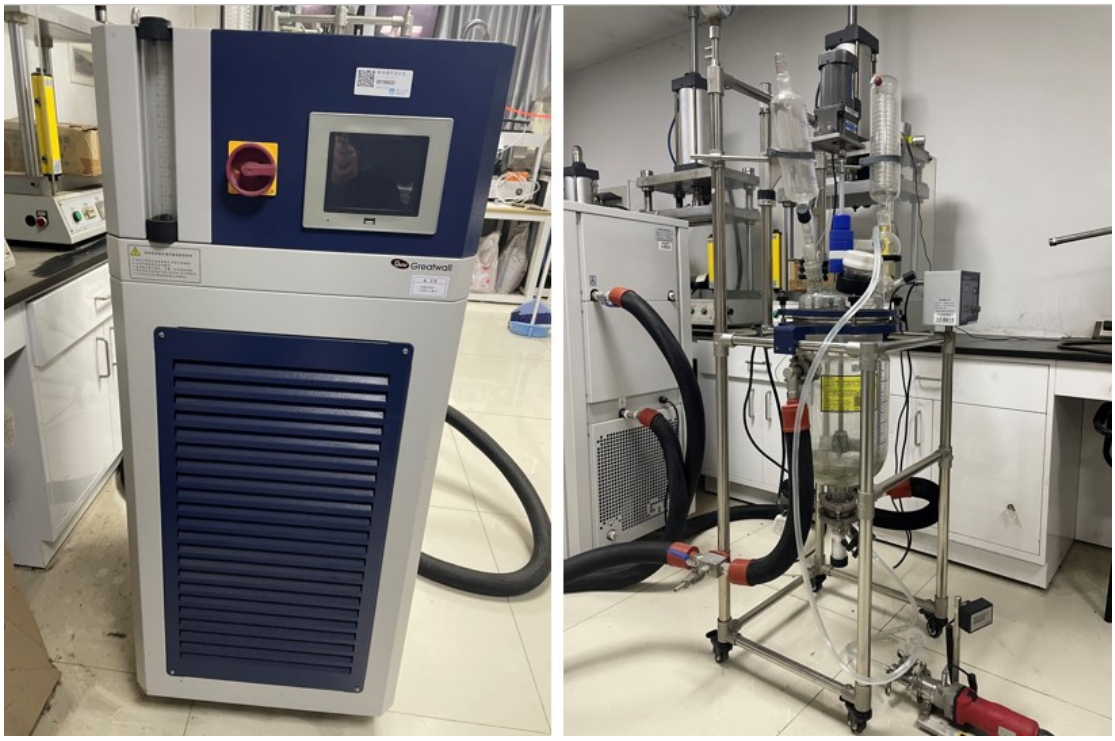

Supplementary Figure.2 $W_{0.02}$-SnO_2 enlarged production equipment

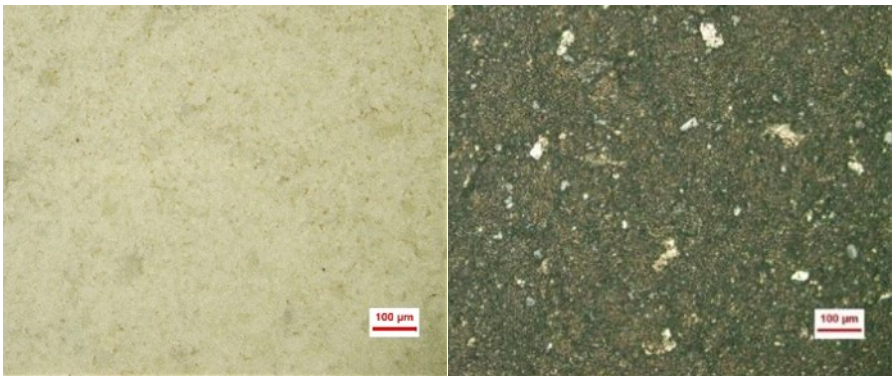

Supplementary Figure. 3 Photograph of the $W_{0.02}$-SnO_2 and Pt/$W_{0.02}$-SnO_2-C catalysis taken by metallographic microscope

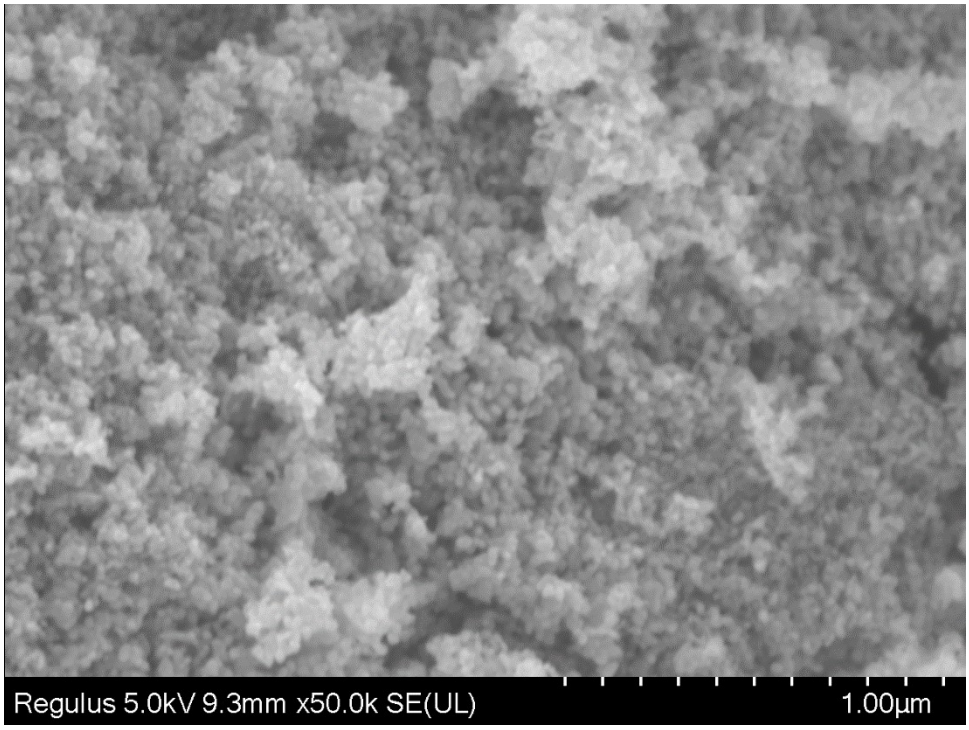

Supplementary Figure. 4 Photograph of the $Pt/W_{0.02}$-SnO_2-C catalysis taken by SEM

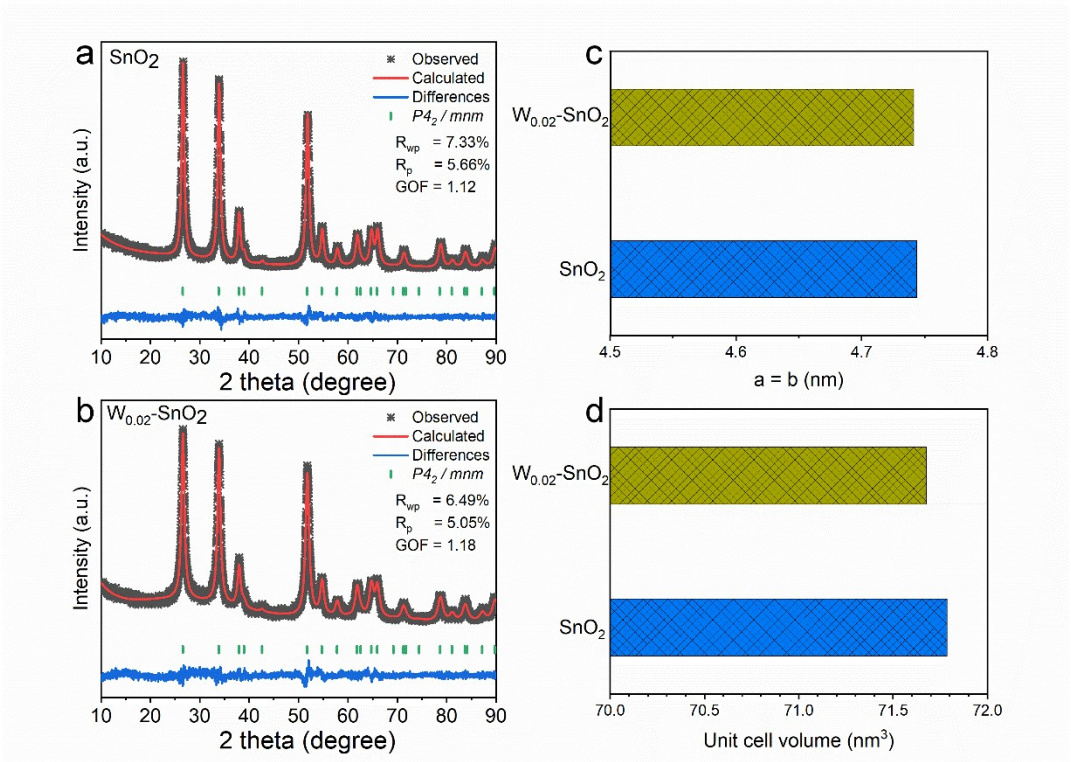

Supplementary Figure. 5 (a-b) XRD patterns of doped and undoped SnO_2 (c) evolution of rutile lattice parameters and (d) evolution of cell volume of rutile.

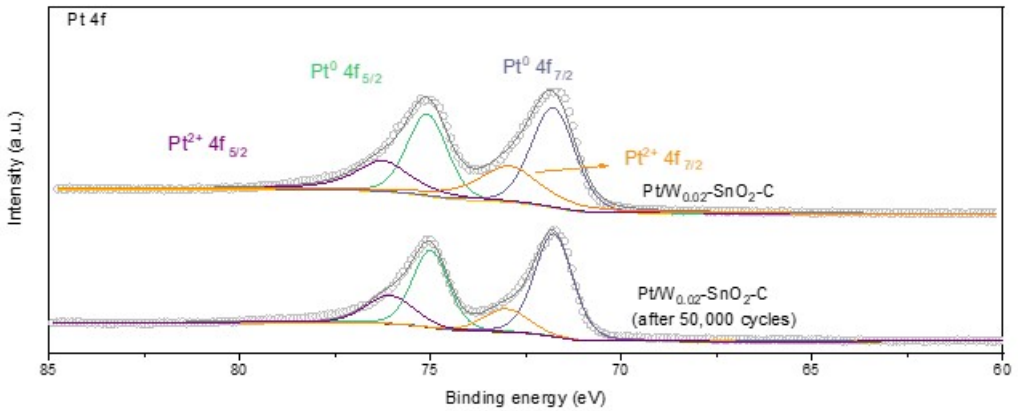

Supplementary Figure. 6 XPS patterns of Pt 4f spectrum (initial sample and after ADT)

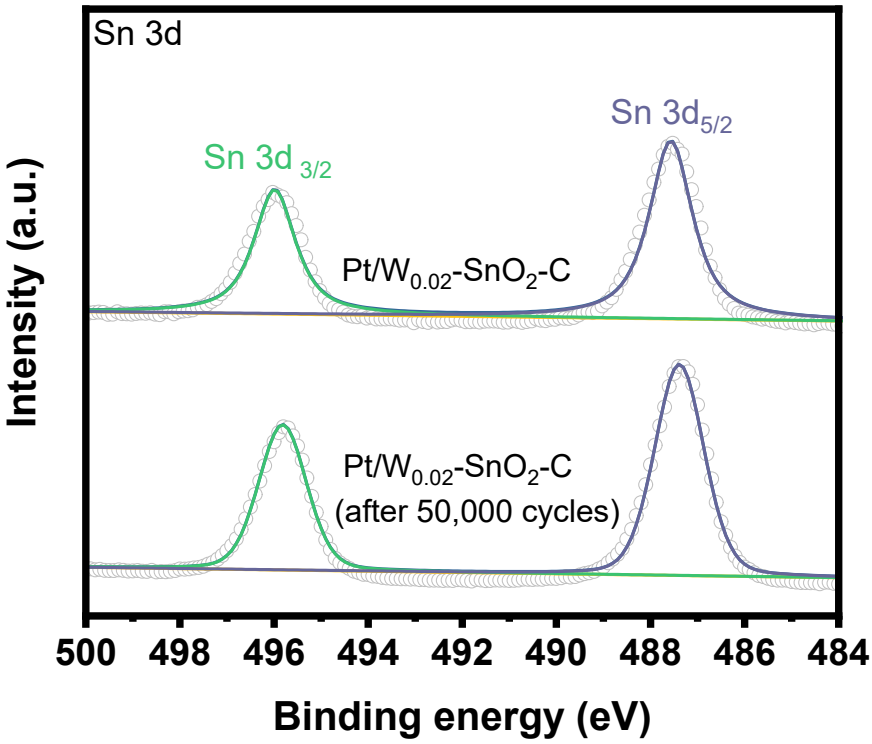

Supplementary Figure. 7 XPS patterns of Sn 3d spectrum (initial sample and after ADT)

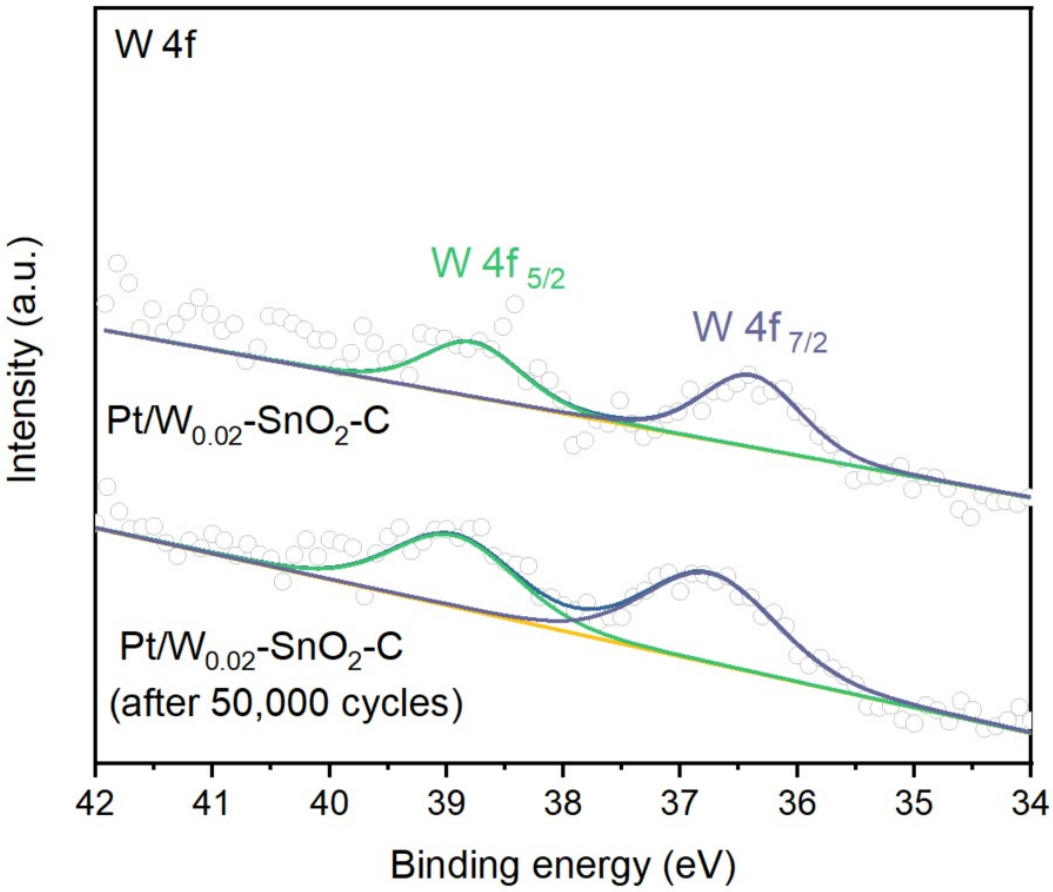

Supplementary Figure. 8XPS patterns of W 4f spectrum (initial sample and after ADT)

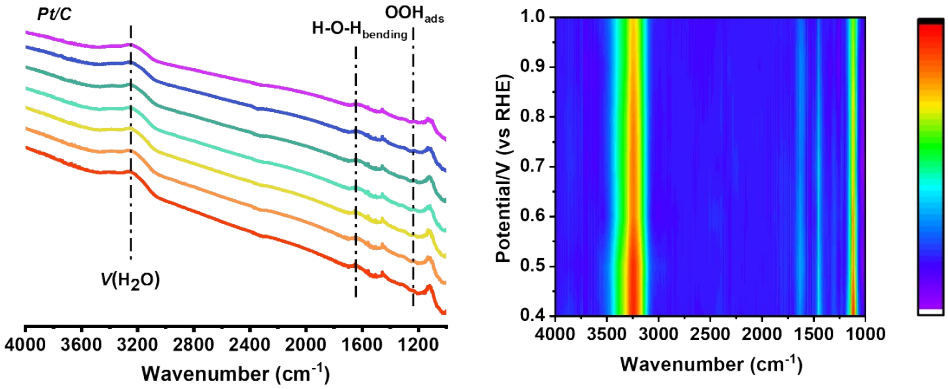

Supplementary Figure. 9 The results of in-situ infrared test on JM Pt/ C

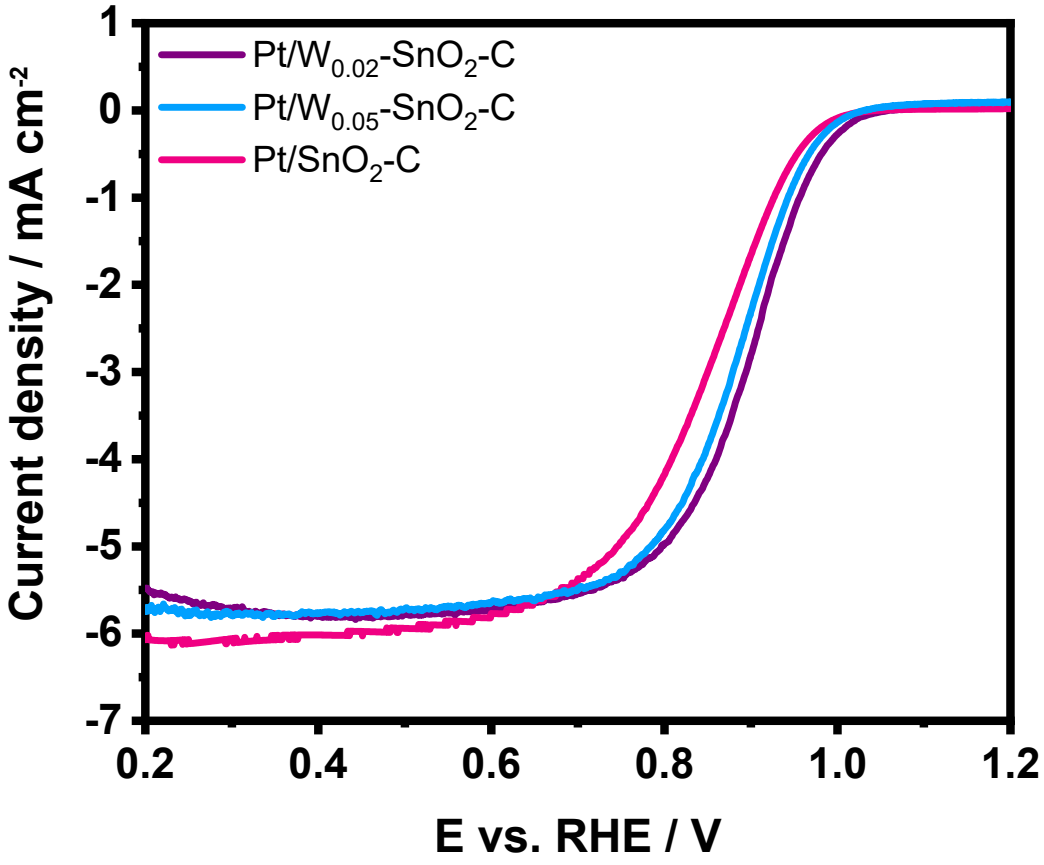

Supplementary Figure. 10 LSV curve of different W doping amounts sample

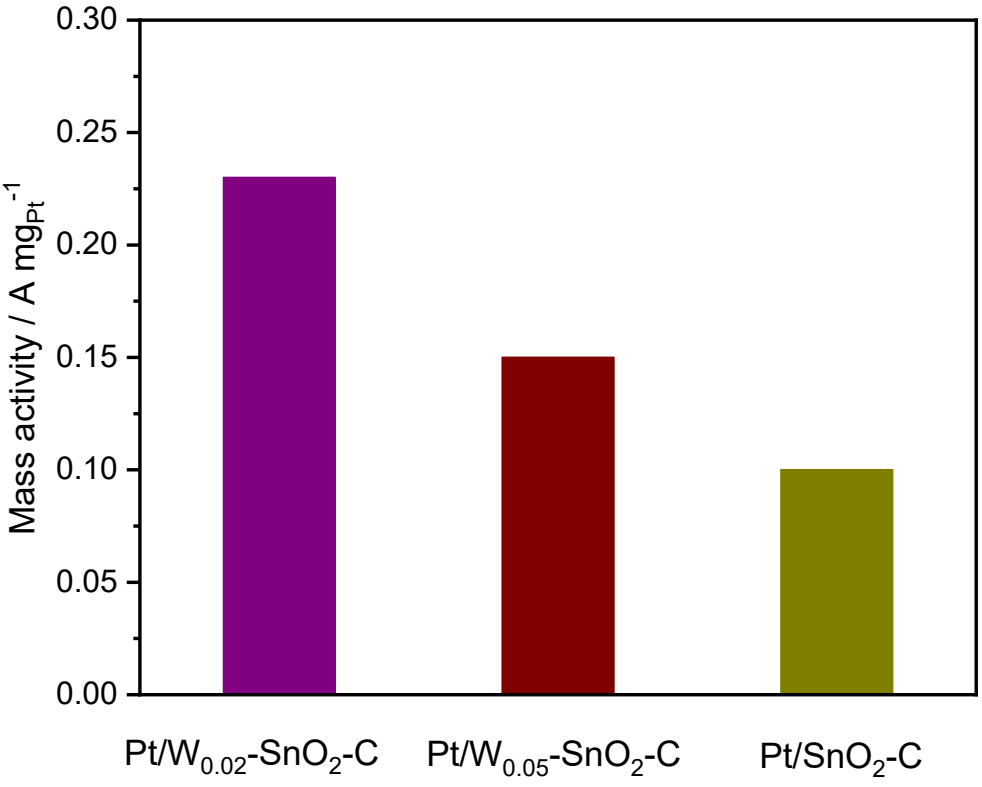

Supplementary Figure. 11 MA of different W doping amounts sample

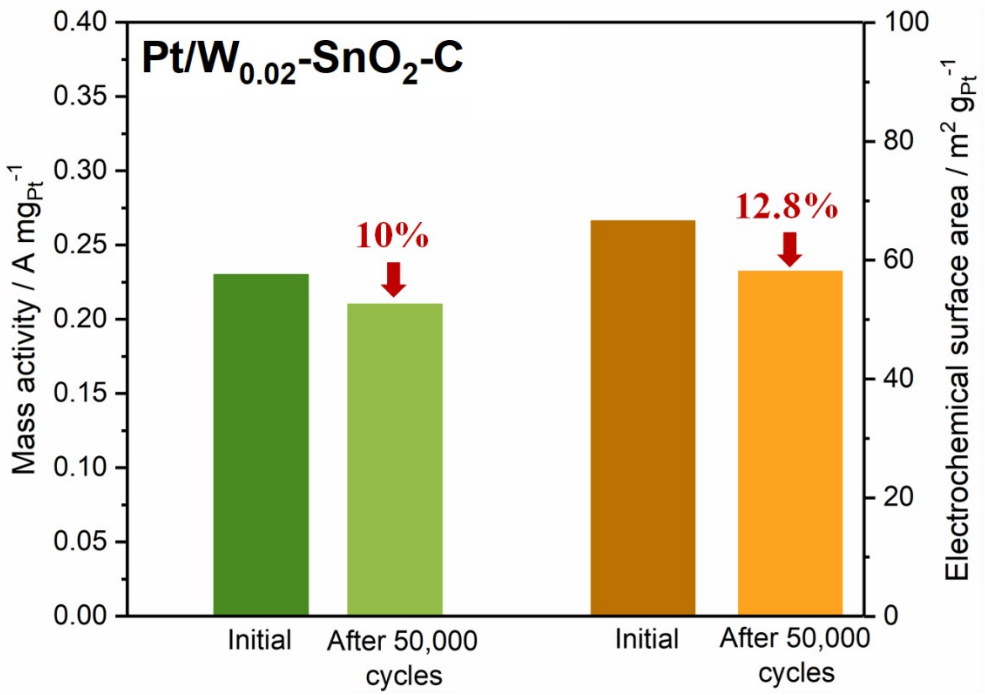

Supplementary Figure. 12 MA and ECSA of $Pt/W_{0.02}$-SnO_2-C after ADT

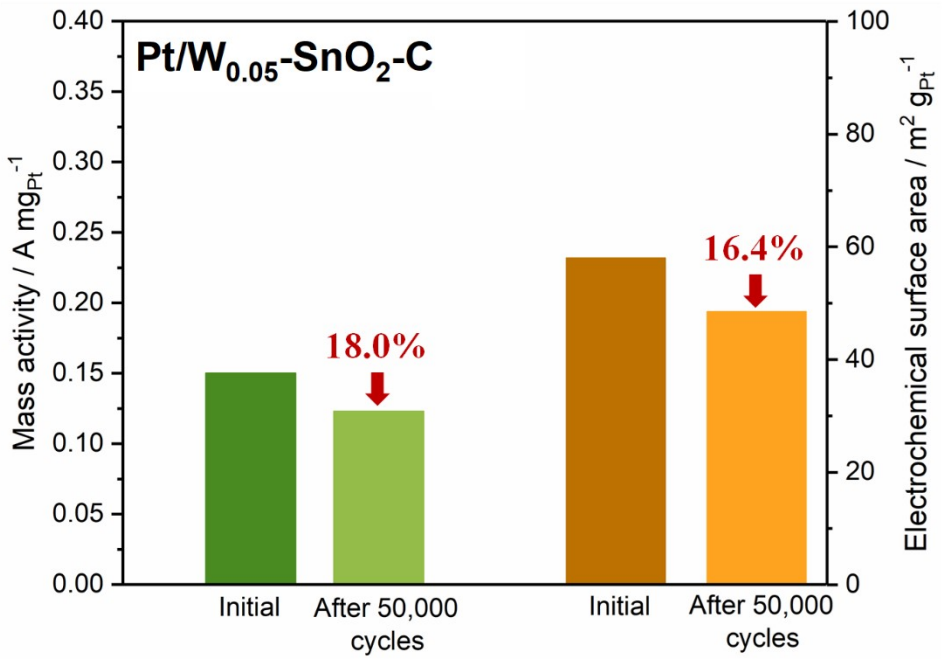

Supplementary Figure. 13 MA and ECSA of $Pt/W_{0.05}$-SnO_2-C after ADT

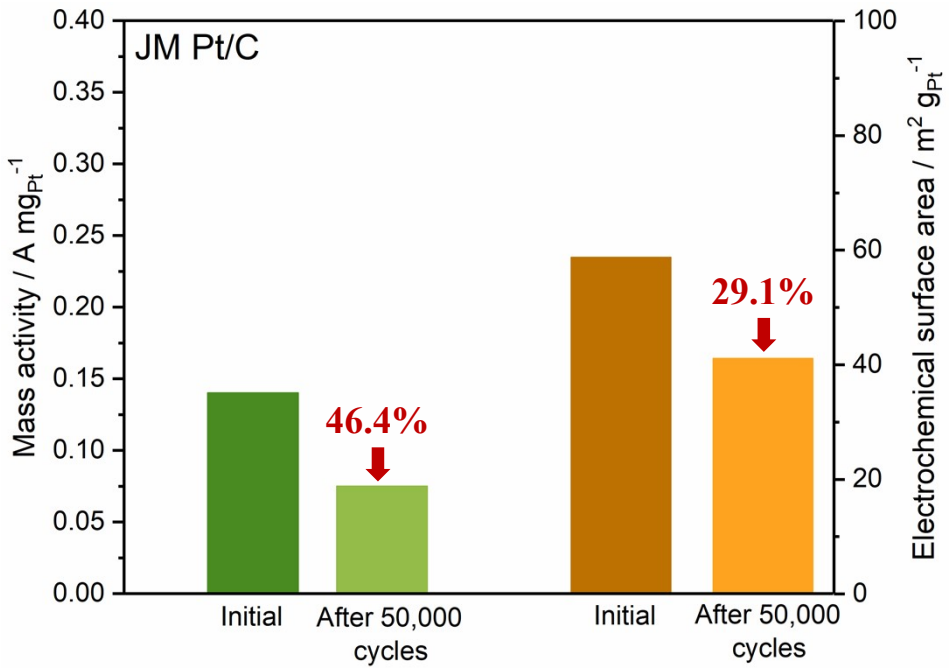

Supplementary Figure. 14 MA and ECSA of JM Pt/C after ADT

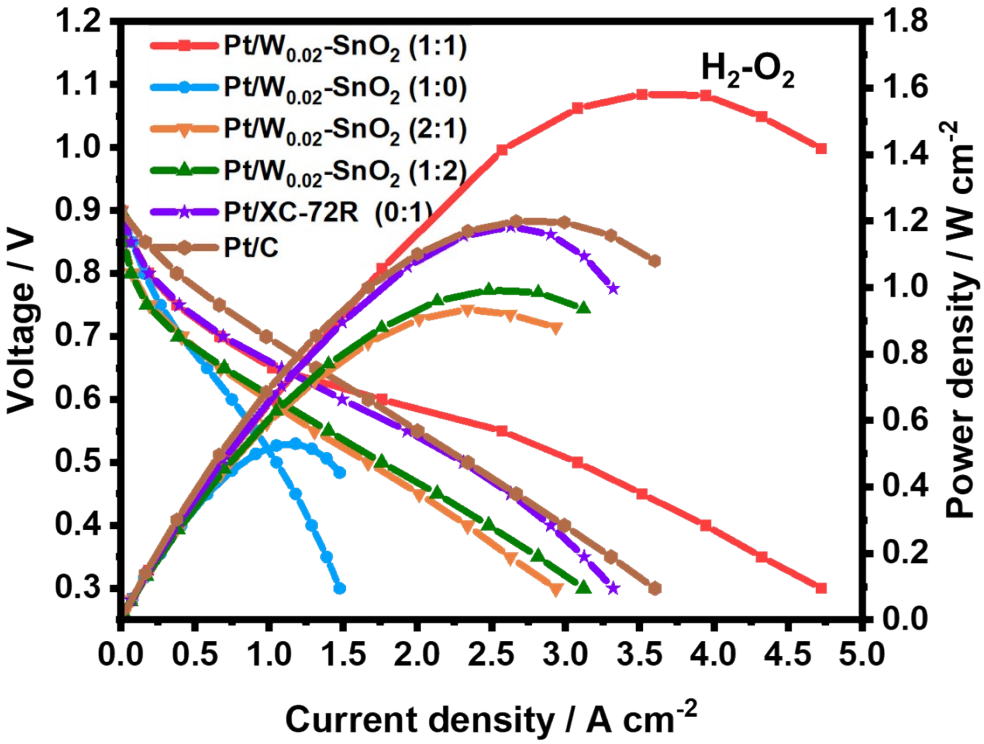

Supplementary Figure. 15 Electrochemical performance of H_2−O_2 single cells for different catalyst samples

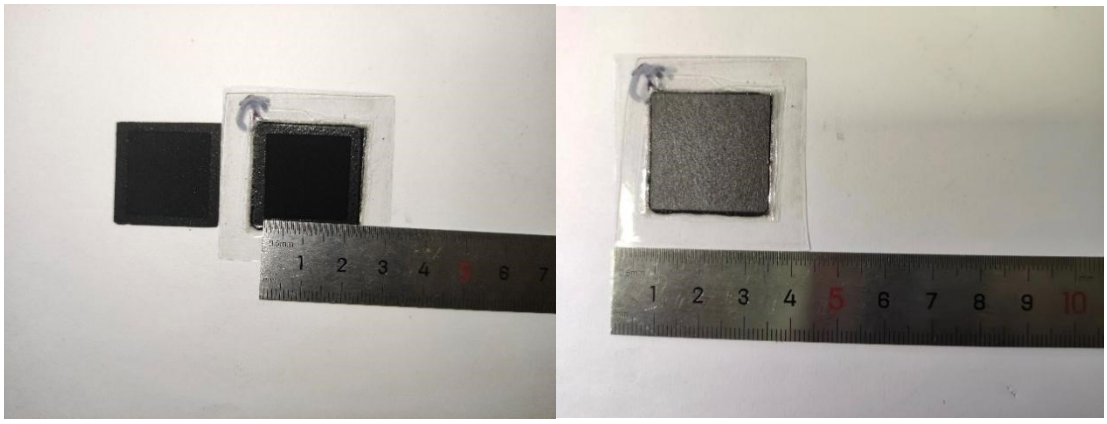

Supplementary Figure. 16 The size of MEA (S =4cm^2)

Supplementary Figure. 17 Ultrasonic spraying machine (Siansonic UC320)

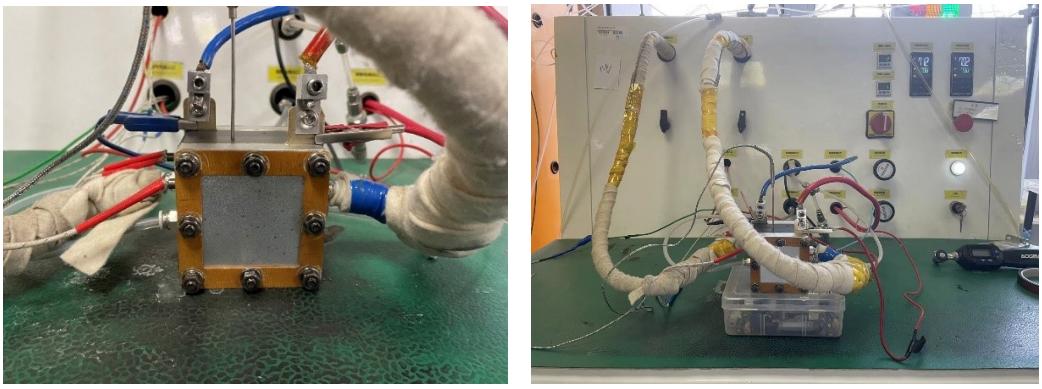

Supplementary Figure. 18 Fuel cell testing machine for MEA

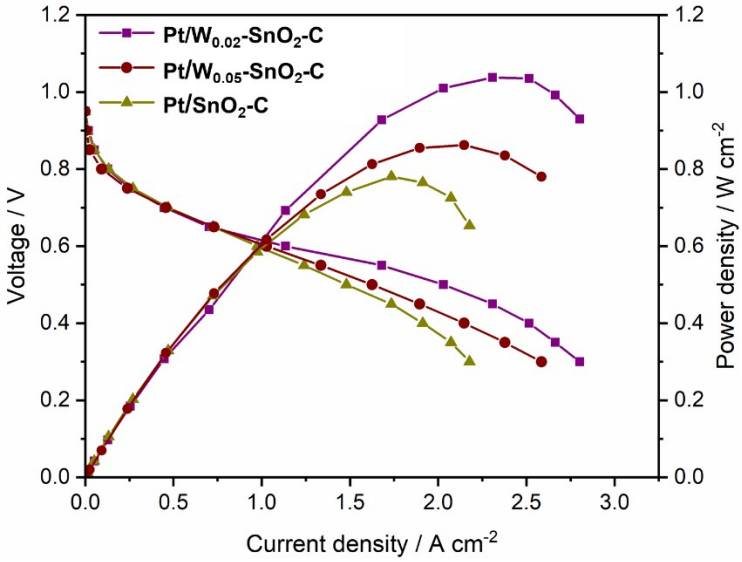

Supplementary Figure. 19 Electrochemical performance of H_2−Air single cells for different catalyst samples (different W doping)

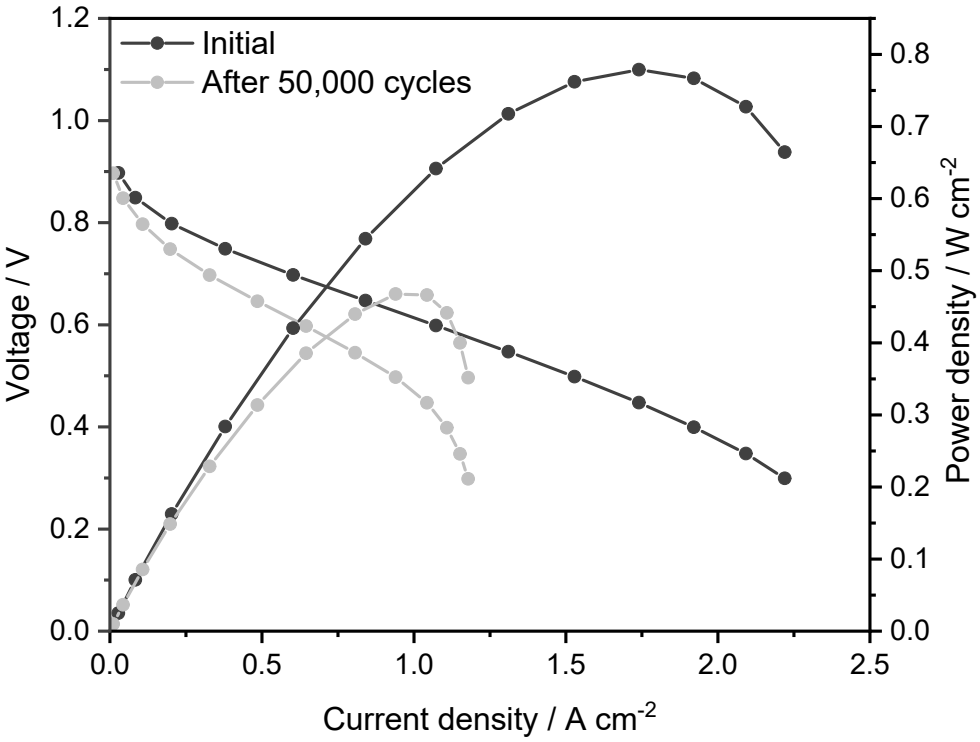

Supplementary Figure. 20 Electrochemical performance of H_2−Air single cells for Pt/C (After ADT)

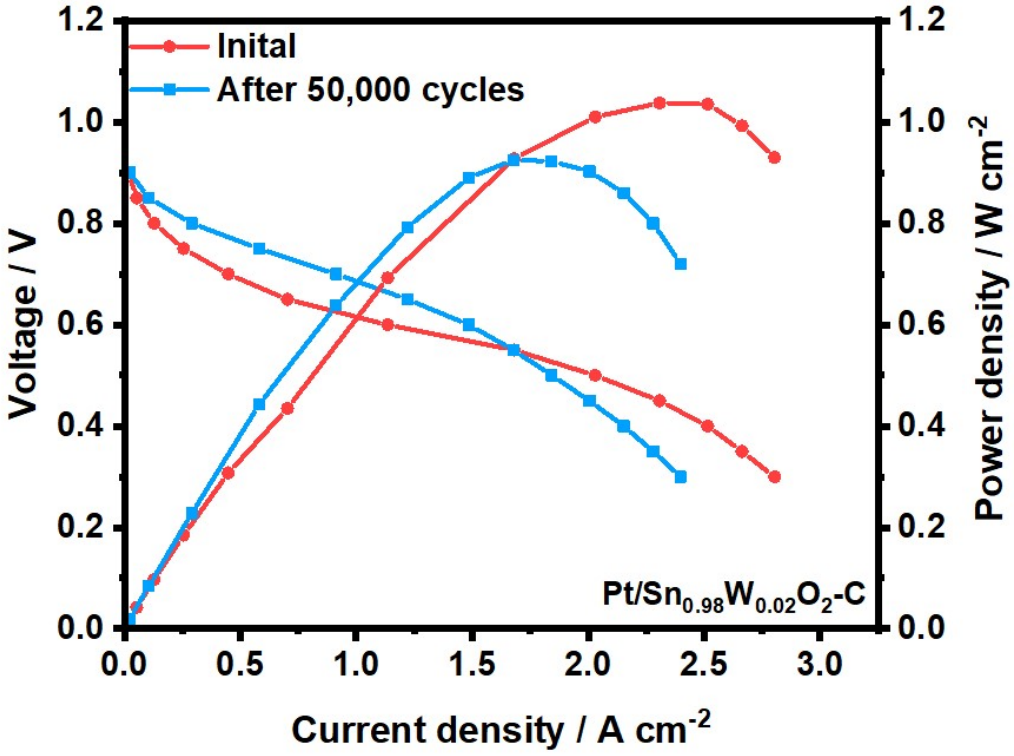

Supplementary Figure. 21 Electrochemical performance of H_2−Air single cells for Pt/$W_{0.02}$-SnO_2-C (After ADT)

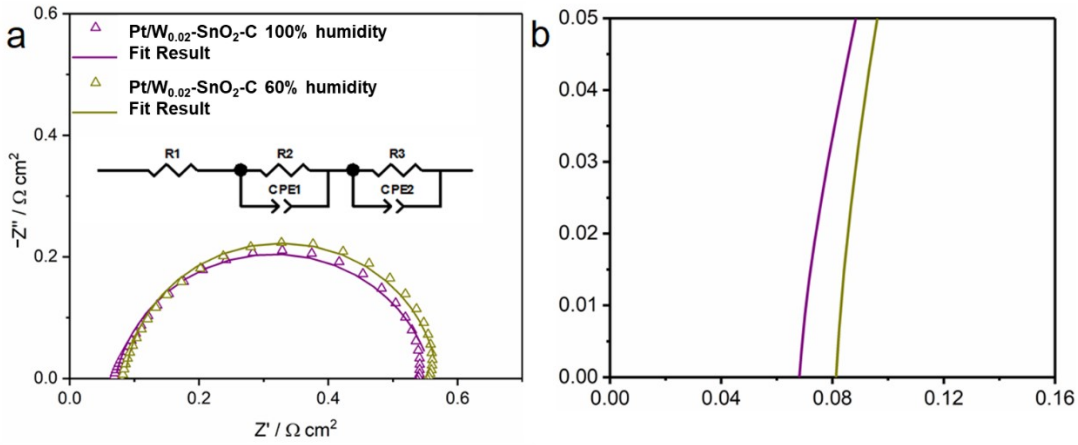

Supplementary Figure. 22 (a) Impedance test result of H_2−Air single cells for Pt/$W_{0.02}$-SnO_2-C (under different humidity), (b) Enlarged view of impedance curve

(Ohmic resistance, charge transfer resistance, mass transfer resistance, and constant phase components associated with double-layer capacitance are represented by R1, R2, R3, and CPE, respectively)

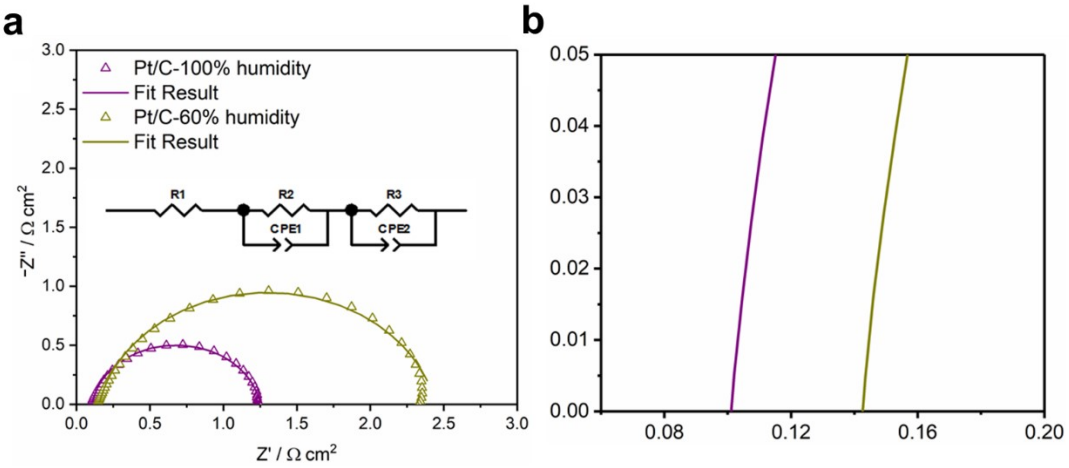

Supplementary Figure. 23 (a) Impedance test result of H_2−Air single cells for JM Pt/C (under different humidity) , (b) Enlarged view of impedance curve

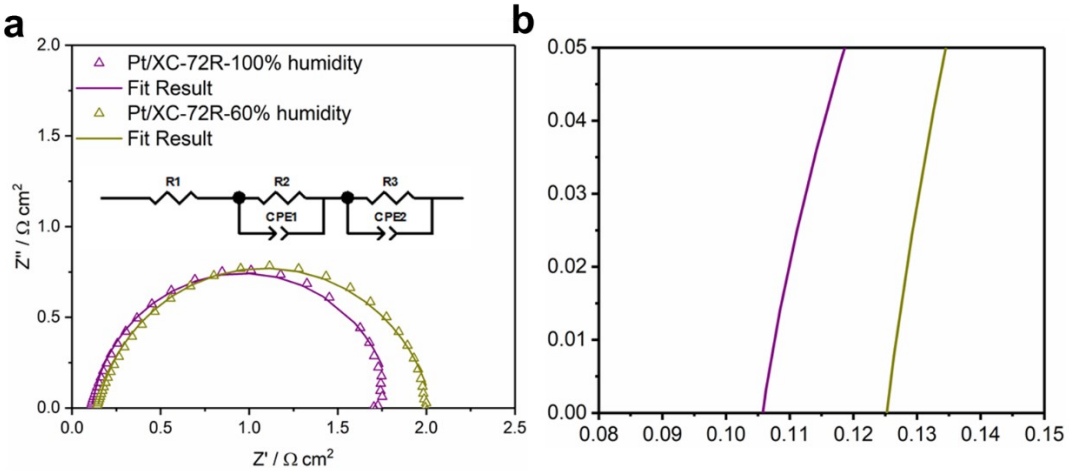

Supplementary Figure. 24 (a) Impedance test result of H_2−Air single cells for Pt/XC-72R (under different humidity), (b) Enlarged view of impedance curve

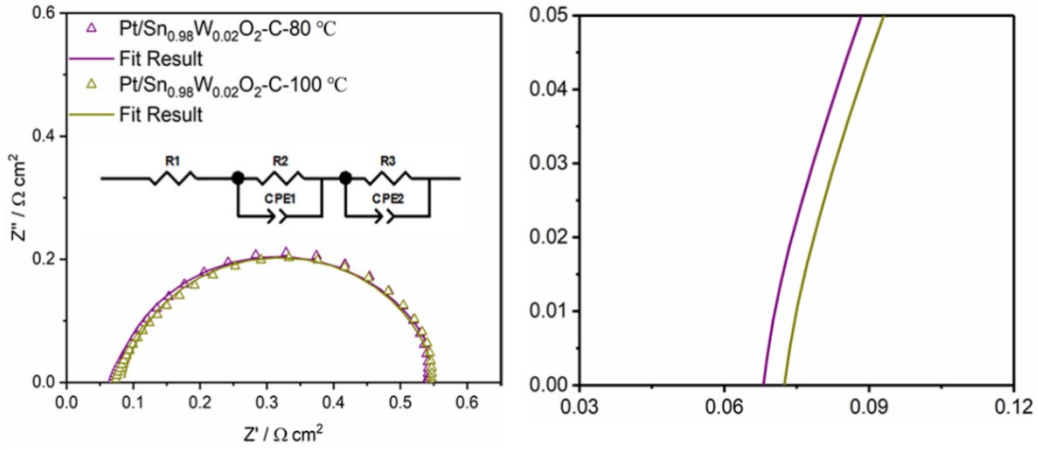

Supplementary Figure. 25 (a) Impedance test result of H_2−Air single cells for Pt/$W_{0.02}$-SnO_2-C (under different temperature), (b) Enlarged view of impedance curve

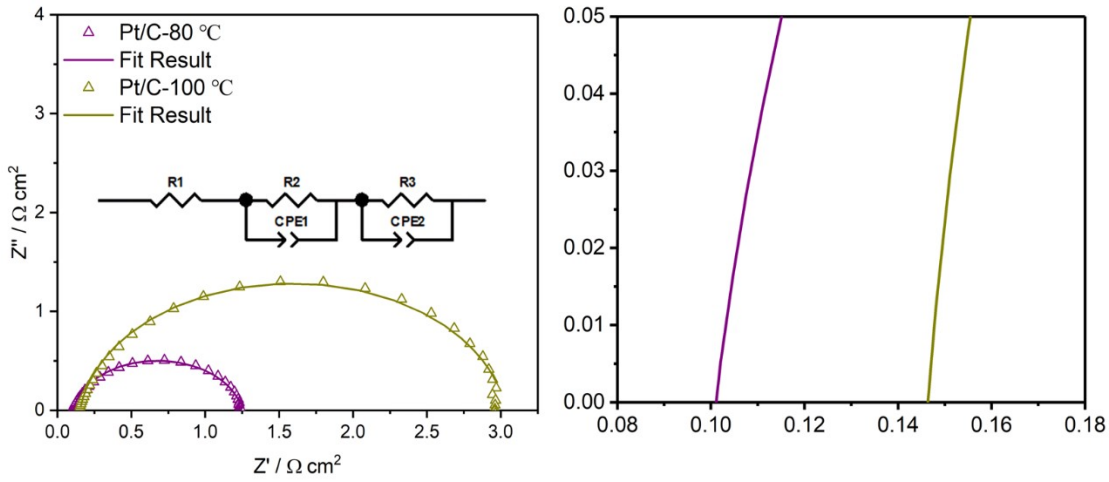

Supplementary Figure. 26 (a) Impedance test result of H_2−Air single cells for JM Pt/C (under different temperature) , (b) Enlarged view of impedance curve

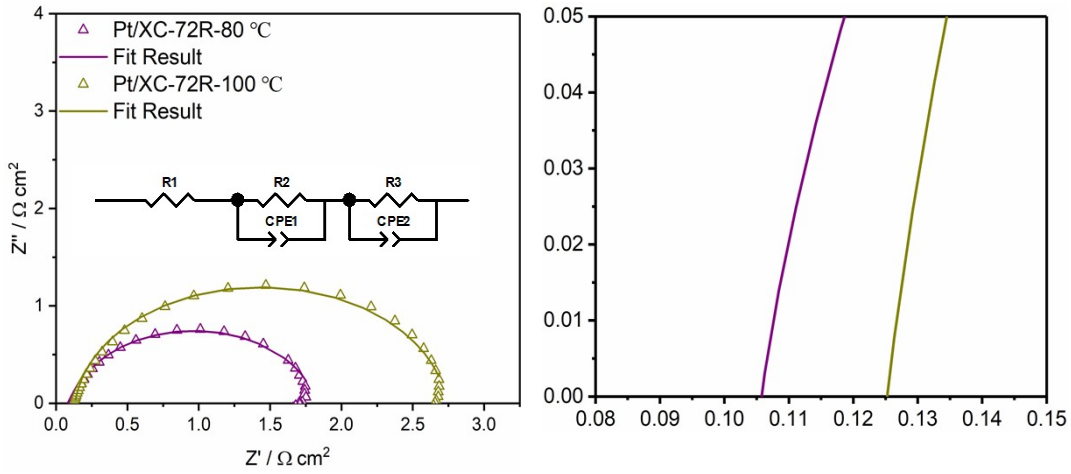

Supplementary Figure. 27 (a) Impedance test result of H_2−Air single cells for Pt/XC (under different temperature), (b) Enlarged view of impedance curve

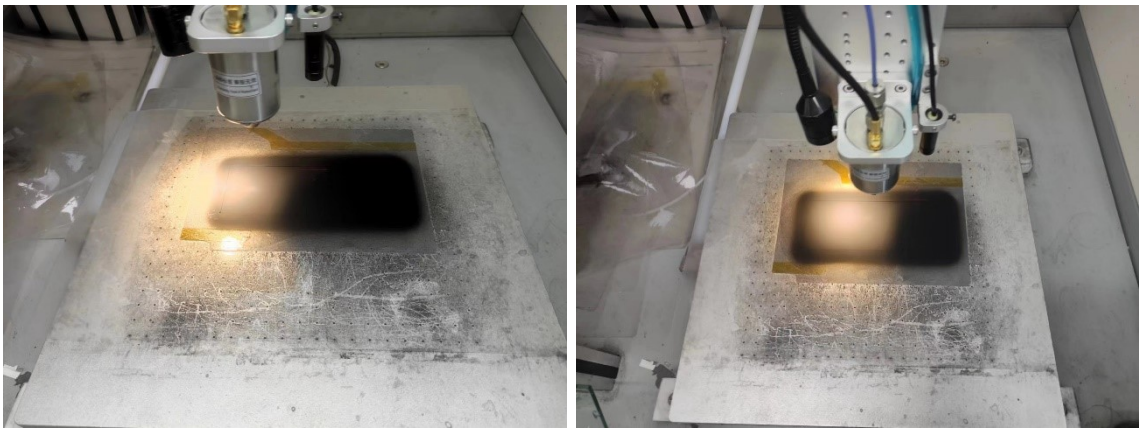

Supplementary Figure. 28 Preparation of large membrane electrodes by ultrasonic spraying (Siansonic UC320)

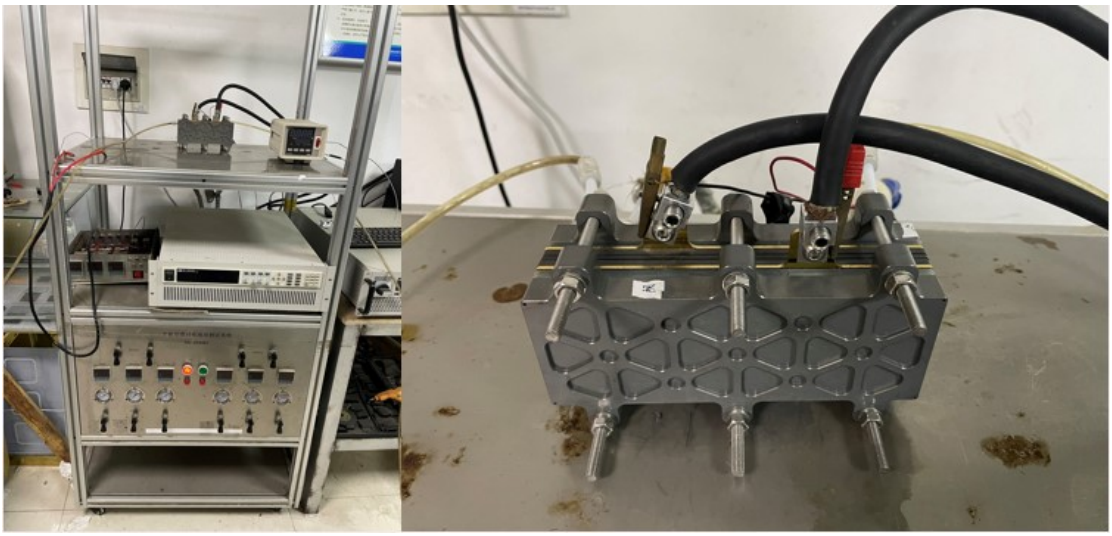

Supplementary Figure. 29 Large fuel cell test platform and the electric pile of $Pt/W_{0.02}$-SnO_2-C

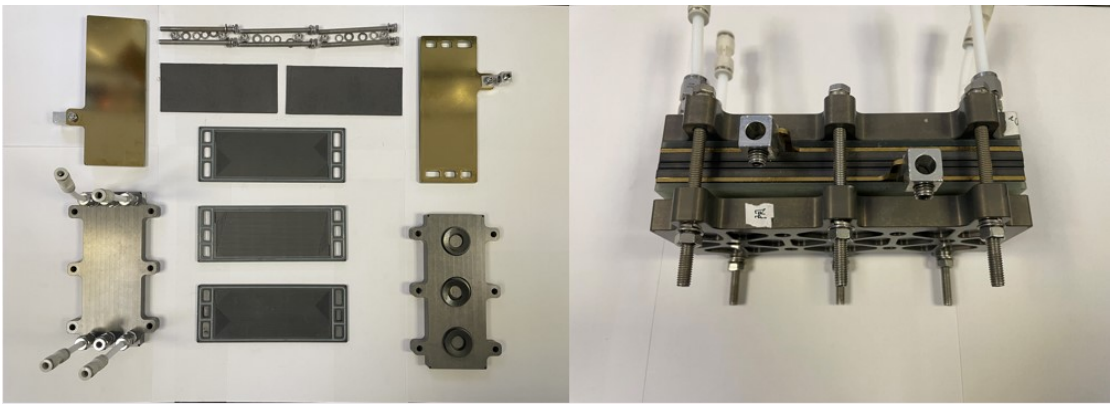

Supplementary Figure. 30 The electric pile parts display and complete electric pile assembly display

Table S1 ICP after ADT of $Pt/W_{0.02}$-SnO_2-C

$Pt/W_{0.02}$-SnO_2-C	Analyte	average value
10000	Sn 189.927	1.432 mg/L
30000	Sn 189.927	5.863 mg/L
50000	Sn 189.927	8.757 mg/L
	Ca 317.933	5.045 mg/L
	Pt 265.946	11.92 mg/L

Electrochemical Measurements

The electrochemical surface area (ECSA) of Pt was determined in the catalysts using the following equations, respectively:

$$ECSA = \frac{Q_H}{0.21 \times [Pt]}$$

where the QH (mC) is the charge due to the hydrogen adsorption/desorption in the hydrogen region of the CVs, 0.21 mC cm^{-2} is the electrical charge associated with monolayer adsorption of hydrogen on Pt, and [Pt] is the loading of Pt on the working electrode.

$$B = 0.62nFC_0(D_0)^{2/3}\nu^{-1/6}$$

Where F is the Faraday's constant (F = 96,485 C mol^{-1}), C_0 is the saturated concentration of O_2 ($C_0 = 1.2 \times 10^{-3}$ mol L^{-1}), D_0 is the diffusion coefficient of O_2 ($D_0 = 1.9 \times 10^{-5}$ cm^2 s^{-1} for 0.1 M $HClO_4$ solution) and ν is the kinetic viscosity of the electrolyte (ν = 0.01 cm^2 s^{-1} for 0.1 M $HClO_4$ solution and).